EXAMINATION OF NITRIC OXIDE FORMATION FOR UNSEEDED MOLECULAR TAGGING VELOCIMETRY

By

William C. Bearden

THESIS

Submitted to the Faculty of the

Graduate School of Vanderbilt University

In partial fulfillment of the requirements

For the degree of

MASTER OF SCIENCE

in

Mechanical Engineering

May, 2017

Nashville, Tennessee

Approved:

Robert W. Pitz, Ph.D.

Amrutur V. Anilkumar, Ph.D.

Carl A. Hall, Ph.D.

To Chris and Steve

ACKNOWLEDGEMENTS

Without the support, guidance, and education provided by Dr. Robert W. Pitz this would not be possible. To him, I direct a heartfelt thanks for steering me through this 2 year long journey in which I have grown so much as a student, a researcher, and a teacher.

I also thank Dr. Carl A. Hall: as a mentor and colleague, there is no equal. Carl is the person who introduced me to experimental research and numerical simulations. To say without him this would not be possible is an understatement of the facts. Thank you.

Thank you, Dr. Amrutur V. Anilkumar. You have been a true teacher both inside and outside the classroom. I have learned lessons from you that will stay with me for a lifetime.

I would also like to acknowledge the help of Dr. Joseph A. Wehrmeyer for his help in experimental setup as well as the use of several pieces of lab equipment.

To Darren Tinker and Chad Carpenter, thank you for the support and commiseration that we have shared over the last 2 years. I am proud to call you friends and colleagues.

I wish to thank the Department of Mechanical Engineering for their financial and administrative support throughout this process. Thank you also to the United States Navy and my chain of command for allowing me and supporting me to undertake this graduate education.

Finally, I thank my friends and family who have supported through my many endeavors. Specifically, thank you to my mother and father for their tireless support throughout life, to my grandfather for his inspiration to become an engineer, to my grandmother for her inspiration to think globally, and to my brother and two sisters. Thanks to Walker and Thom, two of the best friends anyone could ask for.

TABLE OF CONTENTS

Page

LIST OF FIGURES

Figure Page

Nomenclature

PIV	**P**article **i**mage **v**elocimetry
MTV	**M**olecular **t**agging **v**elocimetry
FLEET	**F**emtosecond **l**aser **e**lectronic **e**xcitation **t**agging
HTV	**H**ydroxyl **t**agging **v**elocimetry
LIF	**L**aser **i**nduced **f**luorescence
RELIEF	**R**aman **e**xcitation plus **l**aser-**i**nduced **e**lectronic **f**luorescence
PHANTOMM	**Ph**oto**a**ctivated **n**on-intrusive **t**racking **o**f **m**olecular **m**otion
Nd:YAG	**N**eo**d**ymium-doped **y**ttrium **a**luminum **g**arnet (refers to the lasing medium of an Nd:YAG laser)
VENOM	**V**ibrationally **e**xcited **n**itric **o**xide **m**onitoring
ArF	**Ar**gon **F**luoride laser (193 nm)
SENKIN	Chemical Kinetics with Sensitivity Analysis Simulation Software
SNR	**S**ignal to **N**oise **R**atio

CHAPTER 1: INTRODUCTION

1.1. INTRODUCTION TO LASER BASED VELOCITY MEASUREMENTS

Laser based velocity measurements have been used extensively to nonintrusively study velocity fields in a variety of experimental conditions for many years. PIV methods have been in use for decades and were one of the first laser based methods to measure velocity fields. These particles advect with the flow and can be imaged by light scattering with a laser. The Mie scattering being imaged with a camera can produce velocity vectors based on multiple images separated in time. The particles will have moved in the intervening time causing a displacement that can be measured in pixels on the camera. There are three main issues with PIV in certain applications.

First, the particles must be injected into the flow. This is rarely desirable and sometimes impossible. The method of injection could perturb the flow or be prevented by the test facilities themselves. For example, it would be difficult to inject particles into a rocket engine over the entire profile in order to examine the rocket exhaust plume. Furthermore, even in the instance where injection is possible, it is quite challenging to uniformly inject the seed particles for proper distribution for high quality velocity measurements [1].

Second, the particles may be an issue when investigating the velocity of reacting flows (e.g. in the hot exhaust of a rocket). They can be problematic for two reasons. One, the particles could quench the flame and therefore fundamentally change the phenomenon being investigated. Two, the particles could degrade or be burned up by the high temperature of the flow.

Third, the particle size and density can become problematic. The particles are on the microscale (much larger than the nanoscale of molecules). This can lead to drastically different flow

characteristics than the flow in which the particles were inserted, thus greatly impacting the accuracy of any velocity measurements. If the particles have a much different momentum scale than the surrounding fluid, then they will not accurately follow a streamline. Therefore, careful selection of seed particle for fluid mechanic properties which match that of the flow is critical to successful measurements [1].

1.2. BACKGROUND ON MOLECULAR TAGGING VELOCIMETRY METHODS

MTV methods are a convenient and practical approach for making velocity measurements in flows where PIV is not possible or accurate. More broadly, "MTV is a whole-field optical technique that relies on molecules that can be turned into long-lifetime tracers upon excitation by photons of appropriate wavelength" [1]. A thorough overview was performed by Koochesfahani et al. [3].

The molecular tags in MTV work can either be seeded or unseeded. In seeded methods, the molecules used as tags are either injected into the flow or are derived therein (e.g. photolysis of N_2O to NO, where NO is used as the tag) [4]. This is similar to the injection of particles in PIV and is a drawback to the method. Therefore the unseeded methods are preferable when they can be implemented.

An example of an unseeded MTV method that is popular and has a high degree of applicability in reacting flows is HTV. In HTV, photolysis of water vapor already present in the flow, creates hydroxyl molecules which are used as the tag. The OH is written into the flow along the path lines of a "write" laser which dissociates the water vapor. The created OH pattern (shown as two crossed lines in figure 1b) advects downstream, which can then be imaged by a "read" laser (LIF of the OH or other tag species). This process is shown in figure 1.

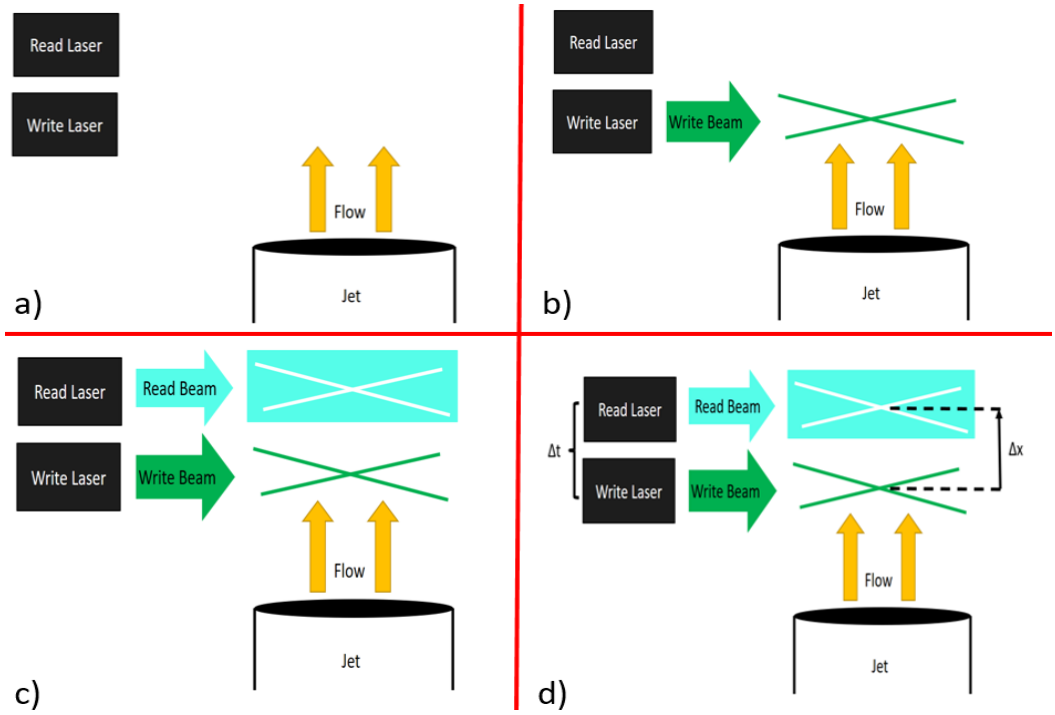

Figure 1: MTV System Schematic. a) flow under study with "write" and "read" laser off, b) "write" laser pulsed and writes lines of tag molecule into flow, c) flow is advected downstream, "read" laser sheet is pulsed illuminating tag lines, d) the distance traveled, Δx, is recorded by a camera over the time difference, Δt, and the resultant velocity is computed, $\frac{\Delta x}{\Delta t}$.

Other methods of MTV are broken down into the method of excitation and imaging which results in the velocity measurement. A thorough overview of these methods can be found in [1]. One of these methods, known as RELIEF, is often used with O_2 molecules. Here, the O_2 is excited to a higher vibrational state which is long lived. This excited state is then imaged by irradiation [5] [6]. A second method, involves the fluorescence of a photoproduct. These methods can be from photolysis (e.g. OH from H_2O) or photosynthesis (e.g. NO from photodissociation of air and subsequent recombination) [7]. The PHANTOMM technique is also included in this type of MTV in which a photosensitive dye is written into the flow and can be imaged indefinitely afterwards proving particularly useful for slow moving flows [1] [8]. FLEET is also part of this group. It utilizes a femtosecond laser in order to electronically excite and dissociate species in the flow regime (usually air or its two main constituents, N_2 and O_2). The excited species are then tracked

by imaging the emission of the species as they return to the ground state. This emission can be due to decreasing energy levels from excited species or from recombination reactions from dissociated species. A good overview of such a method can be found in review by J. Michael et al. [2].

The third MTV method uses phosphorescence of the tag molecule. This method does not need a "read" laser because the excited species (produced by the "write" laser) will continually emit (phosphoresce) photons. For this method to be viable nonradiative energy dissipation pathways cannot be present (and therefore quenching can be an issue). The other requirement is that the emission time scale is sufficiently long to take multiple images of the molecules in order to be able to measure a sufficient displacement for accurate velocity measurements.

In all cases of MTV, accurate distance measurements are crucial in order to have accurate velocity measurements (accuracy of time measurements are not usually an issue because timing is handled by external timing generators). Accurate distance measurements are obscured by spatial uncertainty along the written (and subsequently read) tag line. This can be greatly reduced if a spatial correlation technique [9] is used as well as template matching [10]. In these cases a grid of the molecular tag is formed from intersecting "write" lines. This grid advects downstream and the vertices of the "write" image and the "read" image can be correlated for a two dimensional velocity vector. With multiple cameras, a three dimensional velocity vector can also be resolved. Figure 1 has an example of crossed lines to form a simple grid with one vertex. The displacement of the vertex is labeled Δx. Further information on template matching methods and image processing for increased accuracy can be found at [9] [10].

The final component that must be taken into consideration is the flow's effect on the molecular tag as time increases (after the "write" process). Molecular diffusion of the tag and the dispersion

of the tag by local turbulence both cause spreading of the "write" line as time increases. This is seen clearly in Figure 2 from a study by Brominaar et al. [11].

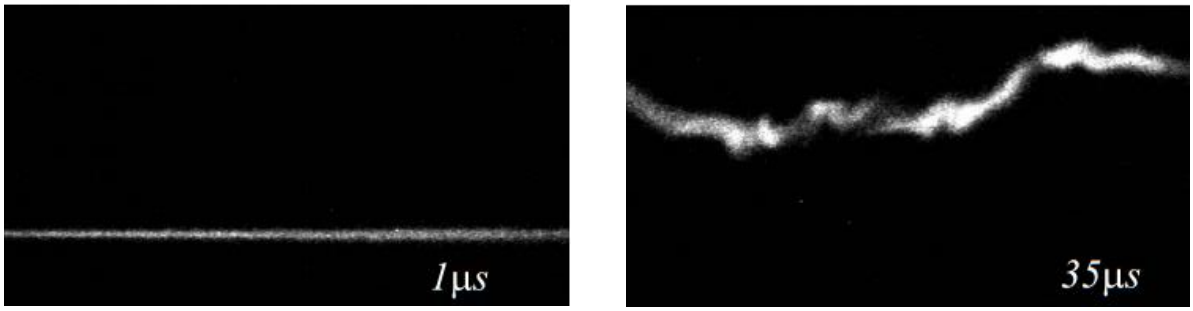

Figure 2: LIF of NO tags written in highly turbulent air at indicated delays after 193 nm excimer "write" laser. Reproduced from study performed by Bominaar et al. *[11]*. The line width of the 35 μs delay image has broadened considerably due to the effects of molecular diffusion and turbulent flow.

1.3. NITRIC OXIDE AS MOLECULAR TAG

The kinetics of NO formation have been studied previously [12]. However, further study with particular application to unseeded MTV is needed, notably, an investigation into the possibility of using a frequency tripled Nd:YAG laser (355 nm output) to produce NO, i.e. as the "write" laser. NO MTV has been studied by using vibrationally excited NO previously. This method has been called VENOM but utilizes seeded NO_2 as the production pathway for the NO (a dissociative process) [13] [14] [15]. VENOM has an advantage of also allowing temperature measurement via comparison of the relative signals of the two different vibrational levels of the NO (at higher temperatures the ratio of the signal strengths of the two levels will skew towards the signal of the higher vibrational level). VENOM is not ideal in all applications due to the reasons previously mentioned. Therefore, it would be advantageous to synthesize NO from unseeded air. The following chemical mechanism for NO production has been proposed [12].

$$N_2 + 3hv_{193nm} \rightarrow N_2^+ + e \quad (1)$$

$$N_2^+ + e \rightarrow N + N \quad (2)$$

$$N + O_2 \rightarrow NO + O \quad (3)$$

The N_2 ionization given by equation (1) has been documented through experimental observation of N_2^+ downstream of a focused ArF excimer laser [12]. Figure 3 illustrates this step on a potential energy plot of different electronic states of N_2. Each 193 nm photon carrying 6.4 eV of energy.

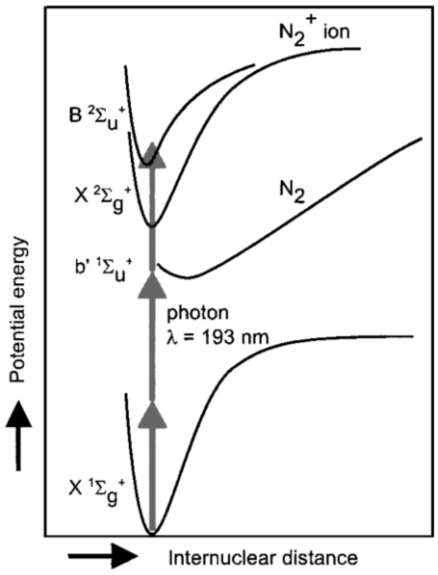

Figure 3: N_2 potential energy curves reproduced from work done by Sijtsema et al. *[7]*. Each arrow represents one photon of 193 nm light.

Moreover, NO has been utilized as a tag for velocity measurements in experimental setups using an ArF laser as the "write" laser first in 2001 [16] and with more success in 2008 [11]. Tag images from these two studies are shown in figures 4a and 4b respectively.

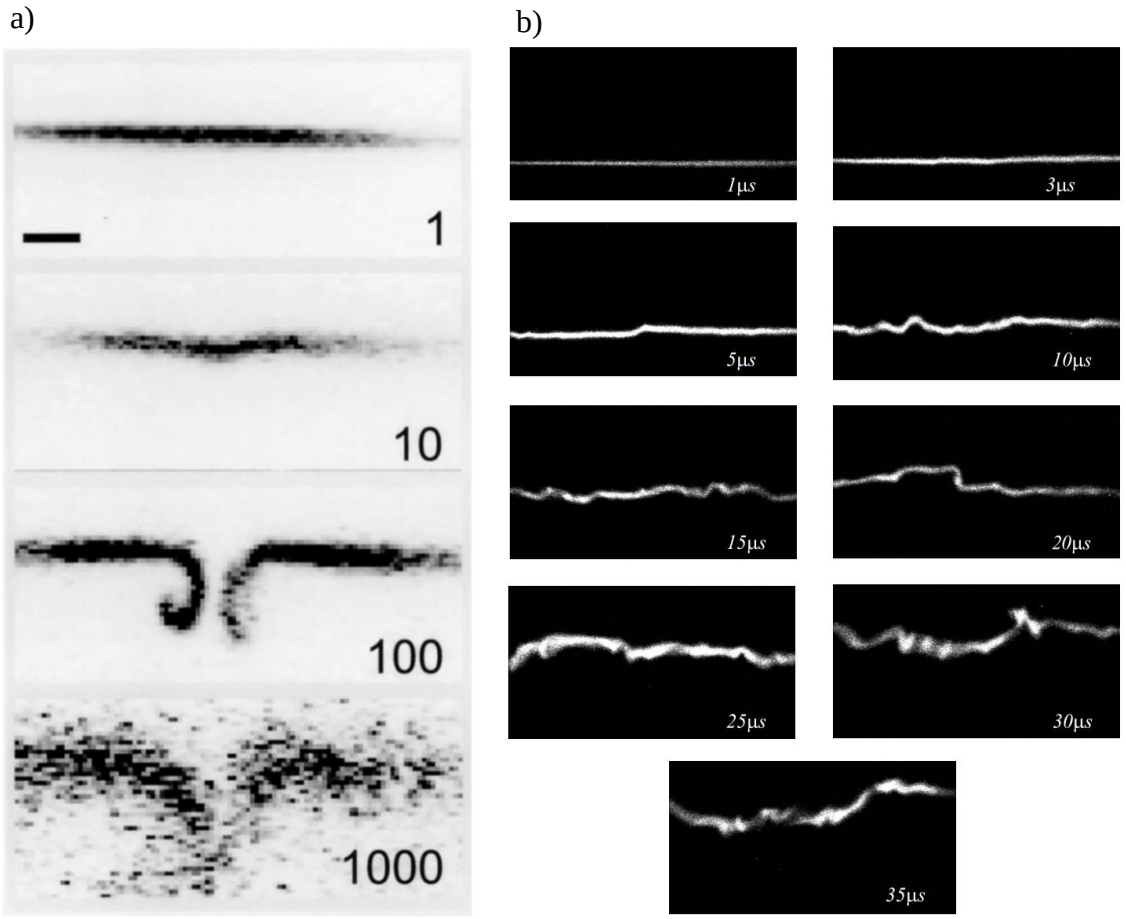

Figure 4: a) is a reproduced set of images from a study by Dam et al. *[16]* of a line of NO written into a pulsed dry air flow at the given time delays between the "write" and "read" lasers in microseconds. The scale in the first image represents 0.5 mm. Each image has been scaled for intensity independently to maximize contrast in each individual image. In b) images are reproduced from a study by Bominaar et al. *[11]* of NO lines written into highly turbulent jet flow. The times indicated are delay times between the "write" and "read" lasers. All lines were "written" into the flow using a 193 nm ArF laser.

The 2008 study [11] showed that the "write" process is highly non-linear, i.e. the concentration of the NO is not related to the intensity of the incident "write" beam linearly. The authors suggest that, given a high enough intensity of light, then the non-linearity can be of great use in the writing of more complex patterns of tag molecule thereby aiding in the measurement of velocity. More complex patterns allow more accurate measurements in more complex flows, specifically turbulent flows. The authors continue this work in [17]. The difference in the quality of the two sets of

images in figure 4 is attributable to a more refined experimental setup in the second study. The latter study [11] used a custom composite focusing lens which achieved a “write” beam waist of 50 μm compared to the ≈180 μm waist of the beam from the first study. The higher intensity of light in the second study paired with the non-linear write process produced much more NO and therefore higher quality images. Please note that the laser power of the “read” and “write” lasers were comparable between the two studies.

This thesis examines the feasibility of replacing the 193 nm ArF excimer laser with a focused 355 nm frequency tripled Nd:YAG laser for the N_2 ionization step. A tripled Nd:YAG has many advantages over the ArF excimer including that it is a solid state laser. It does not require a gas mixture as a lasing medium and the associated maintenance and start up procedure inherent with such a laser. Furthermore, the ArF laser requires dangerous fluorine gas, which requires more safety precautions and procedures for storage, transportation, etc. than the Nd:YAG laser. The Nd:YAG produces a higher quality beam than that of an ArF excimer laser. Also, an Nd:YAG is much more versatile than an ArF laser because, when coupled with a dye laser and wavelength extender, an Nd:YAG has a very wide wavelength output range (ultraviolet to infrared light) and can operate at higher repetition rates (higher repetition rates come at the cost of energy/pulse). These advantages mean that more test facilities already have or would be open to utilizing an Nd:YAG system compared to an ArF excimer. However, these advantages are meaningless without the ability to create NO in sufficient quantities with 355 nm light. If an Nd:YAG system is not comparable or better than the performance of the previously studied ArF systems, then the system will not be useful for experimental work.

The main challenge to the 355 nm excitation scheme is the non-linearity of the method. The previous work performed by Dam, Bominaar, et al. [7] [11] [16] [17] demonstrated the non-

linearity of the 193 nm excitation method (a proposed 3 photon process). They were able to achieve the results in figure 4b with a 50 μm diameter beam. The mechanism proposed herein would be more non-linear as it would require even more photons to achieve the same N_2 ionization in large enough numbers (a 355 nm photon having less energy than a 193 nm photon). Therefore the goal of this investigation is to determine if NO tags can be produced by 355 nm light focused in air with comparable SNRs to the ArF NO production pathway.

CHAPTER 2: SIMULATION OF TAG KINETICS

2.1. INTRODUCTION TO SENKIN

SENKIN is a program that solves time-dependent chemical species concentrations based on provided initial conditions and for a given chemical mechanism comprised of chemical reactions and their associated rate parameters. In addition, SENKIN offers a sensitivity analysis to show which rate parameters are most sensitive to adjustment in terms of a selected final parameter (e.g. the concentration of NO). SENKIN can simulate many scenarios maintaining various states constant (i.e. constant temperature and pressure, or adiabatic and constant pressure, or adiabatic and constant volume, etc.). The governing equations (conservation of mass and energy) are described in more detail elsewhere [18].

2.2. SENKIN RESULTS

The reaction mechanism used for these reaction studies were the Yetter-air mechanism (27 species, 109 reactions) [19] and the H_2-air plasma mechanism from Ohio State (53 species, 200 reactions) [20]. The two mechanisms compare favorably and the results from the Yetter analysis are presented below in figures 5-10.

Figure 5 shows the minority species if there is assumed dissociation of N_2 leading to 1% N_2^+ (this would correspond to just over 1% dissociation of N_2). The previously proposed mechanism for NO production listed in equations 1, 2, and 3 remain largely unchanged. However, equation (1) is slightly modified for the incident photon energy and the mechanism is as follows:

$$N_2 + 6hv_{355nm} \rightarrow N_2^+ + e \quad (4)$$

$$N_2^+ + e \rightarrow N + N \quad (2)$$

$$N + O_2 \rightarrow NO + O \quad (3)$$

The three photons of 193 nm light are replaced by six photons of 355 nm light to achieve the same end. One percent dissociation of N_2 has been observed in the previous method (193 nm excitation) [12] and is therefore chosen as the starting point for this analysis. It is readily clear from the simulation (figure 5) that the excited N_2^+ state is a short lived ion and quickly recombines to form atomic N. Equation (2) is therefore not the rate determining step in the production of NO. Instead, equation (3), the reaction of N with O_2 is slow, resulting in the NO production taking 10000 times longer than that of the recombination. These results of NO formation agree with prior work [11] where the authors imaged NO at several intervals between 1 and 35 µs and found peak intensity (corresponding to peak levels of NO) at ≈ 5 µs.

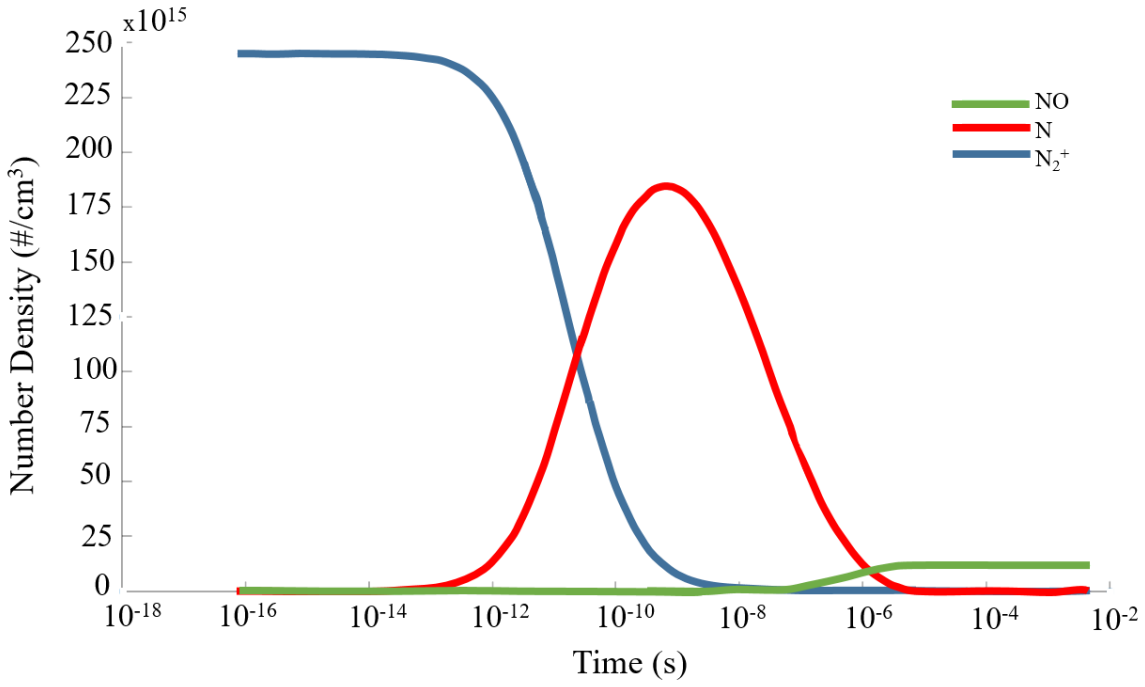

Figure 5: Concentration of minority species in time for 1% dissociation of N_2 in 1 atm, 300 K air. N_2^+ is predicted to be completely consumed by 1 ns, while the atomic N is peaked at this time. Only after 1 µs is the NO predicted to form at appreciable levels, reaching a steady state value at ≈ 5 µs. Simulation was performed utilizing SENKIN as discussed in preceding paragraph with initial conditions of 1% of the present N_2 being ionized to N_2^+. This level of N_2^+ is assumed. The excitation efficiency of 355 nm cannot be simulated with SENKIN, only the chemical kinetics.

In order to gain a fuller understanding of the relationship between percent ionization of the present N_2 on the NO production, further models were run to compare different ionization levels, shown in figures 6 and 7. Simulations were performed with initial conditions of air at 1 atm and 300 K.

The simulations reveal a nonlinear dependence between ionization levels and NO production (figure 8). In other words, NO production does not scale with the amount of atomic N produced by the initial dissociation. Therefore, the created atomic N is consumed via other pathways, for instance recombination reaction to form N_2. The implications of the simulation are that an ionization threshold needs to be met before significant NO begins to form. This threshold will be discussed later and is dependent on the SNR of the experimental system.

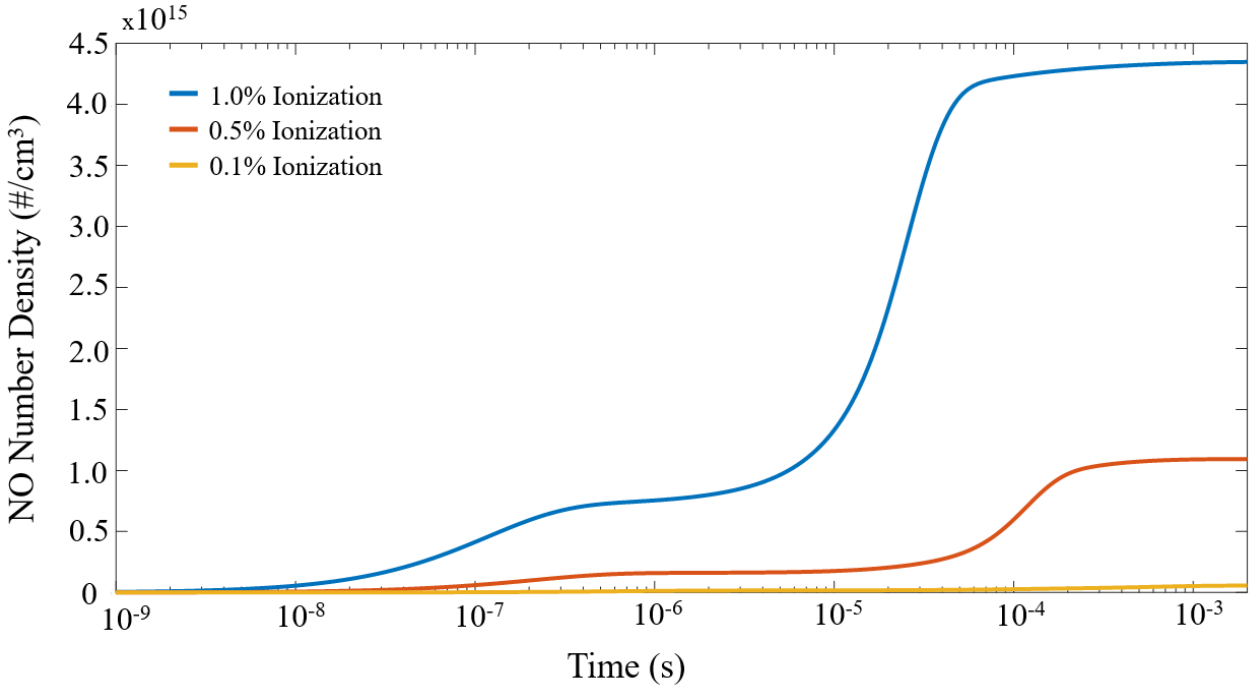

Figure 6: Number density of NO versus time as a result of initial N_2 ionization of 0.1%, 0.5% and 1%. There is an initial plateau centered at 1 μs followed by a steady state value achieved at approximately 100 μs. All simulations performed at 300 K and 1 atm.

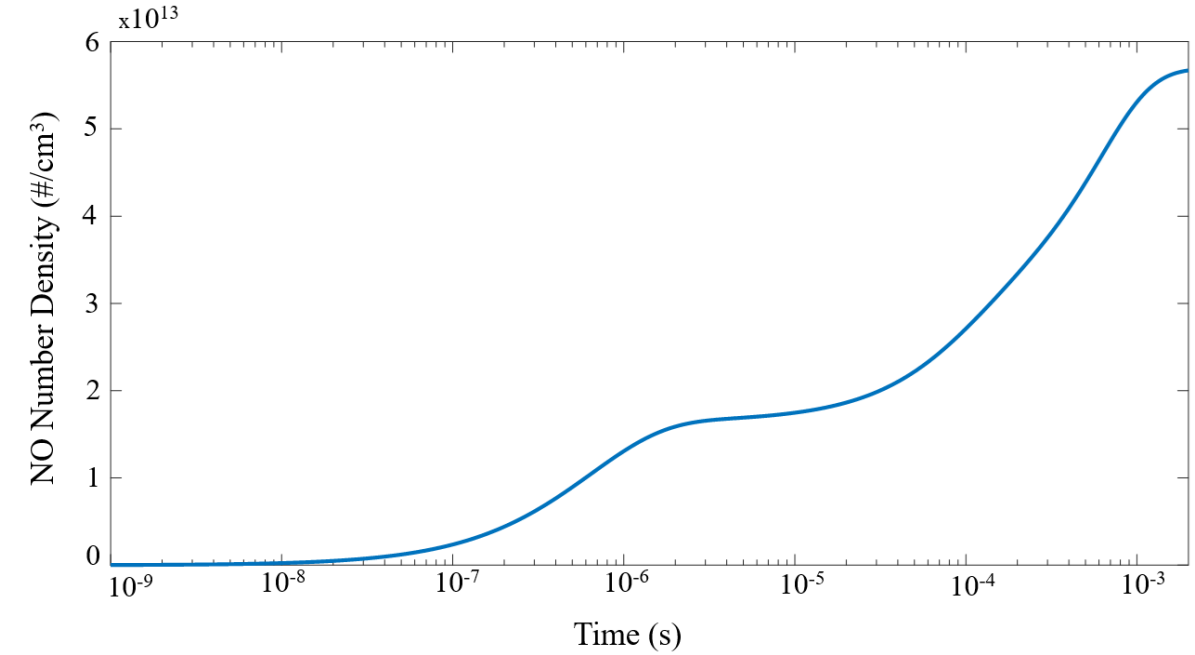

Figure 7: Enlarged image of the 0.1% N_2 ionization curve from 1 μs to 1 ms from Figure 3. The plateaued regions are not as pronounced and shifted in time to the right (a later time). Simulation at 300 K and 1 atm.

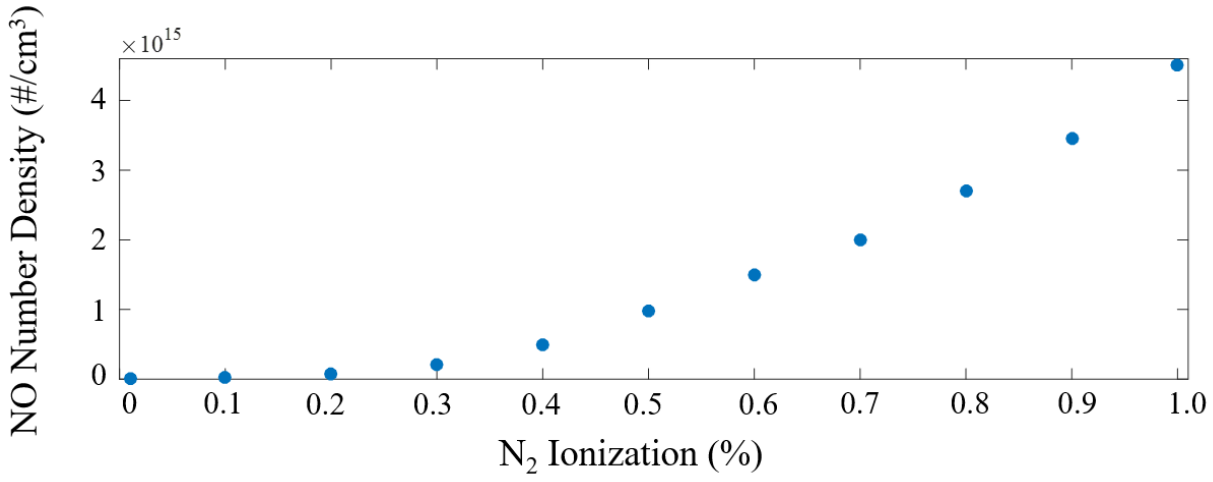

Figure 8: NO number density dependence on N_2 ionization level simulations at 300 K and 1 atm. As previously stated, NO formation has been experimentally observed as non-linear in 193 nm excitation studies. The simulations performed also show non-linear dependence on the levels of N_2^+ ions produced. NO levels are taken at 1 ms of the simulations.

In addition to ionization dependence, the chemical kinetics are likely to be highly dependent on pressure. There are two ways in which pressure should impact the chemical kinetics. One, at higher pressures the molecular collisional rate is increased. Molecular collisions are the vehicle by which chemical reactions take place and therefore added collisions should accelerate the formation of NO but also its destruction. Two, increased pressure increases the number density of the N_2 present in the beam volume of the "write" laser. This should increase the number of N_2 molecules which are ionized, increasing NO production. In other words, if 1% ionization can be achieved, then 1% of the molecules present in a given volume at 10 atm of pressure is much greater than the 1% of molecules in the same volume at 1 atm of pressure. This logic is limited by the total laser energy which has a finite number of molecules it can excite before all the energy of the pulse has been consumed.

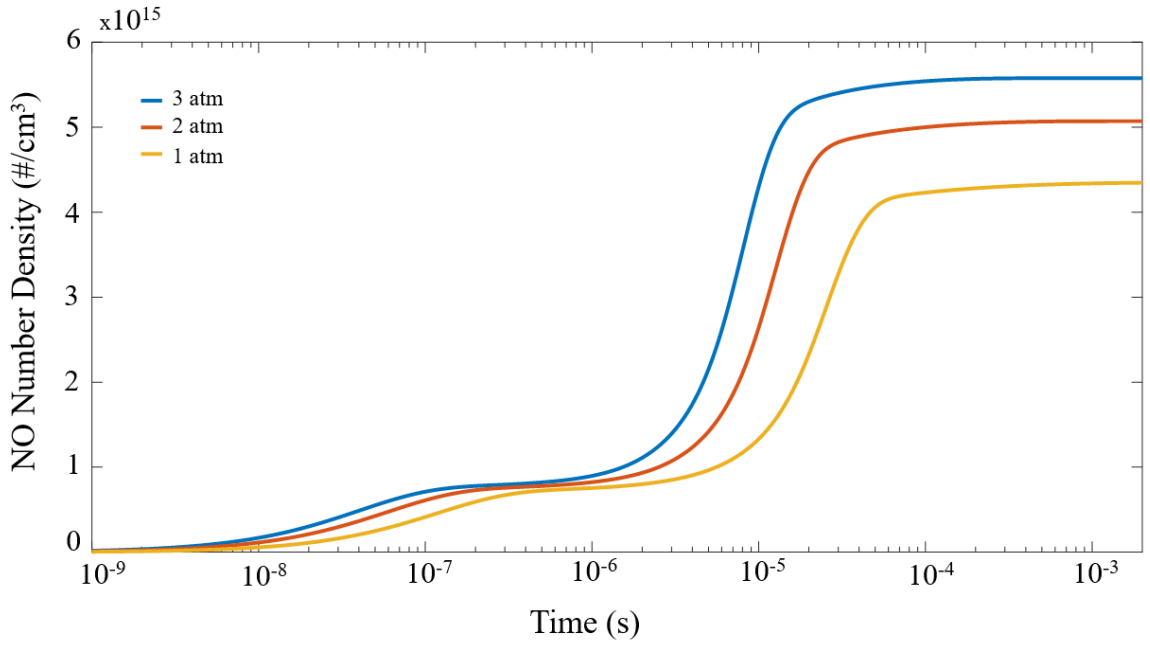

Figure 9: Pressure dependence on NO formation is examined. With the long lifetime of NO, the pressure does not have an appreciable effect on lifetime, but enhances the NO concentrations. In these simulations, ionization was held constant at 1% of present N_2 and temperature at 300 K.

Based on kinetic theory, the simulations should therefore show 1) faster formation rates for higher pressures, 2) higher total NO number density, and 3) shorter lifetimes with increased pressure. Results for three different pressures are plotted in figure 9 against time.

The first two predictions are observable in the plots. The third prediction of shorter lifetimes is not present due to the limited time frame of the simulations. Each simulation was only run for 2 ms, a sufficient time for any MTV work. Due to the molecular stability of NO, the shortened lifetimes at higher pressures are not a concern for this MTV work. NO has been imaged as far as 10 ms after “writing” in prior work by Sijtsema et al. [7]. At these time scales, the predominant factor will not be whether the NO has been destroyed but the impact of diffusion of the tag over such a long period of time.

Below, in figure 10, a direct correlation between NO concentration and pressure is plotted. All the simulated data points are taken at 1 ms in time. The percent ionization is maintained constant for all 10 simulations at 1%. This presupposes the laser has enough energy and the excitation scheme is efficient enough to run at 1% ionization at 10 atm.

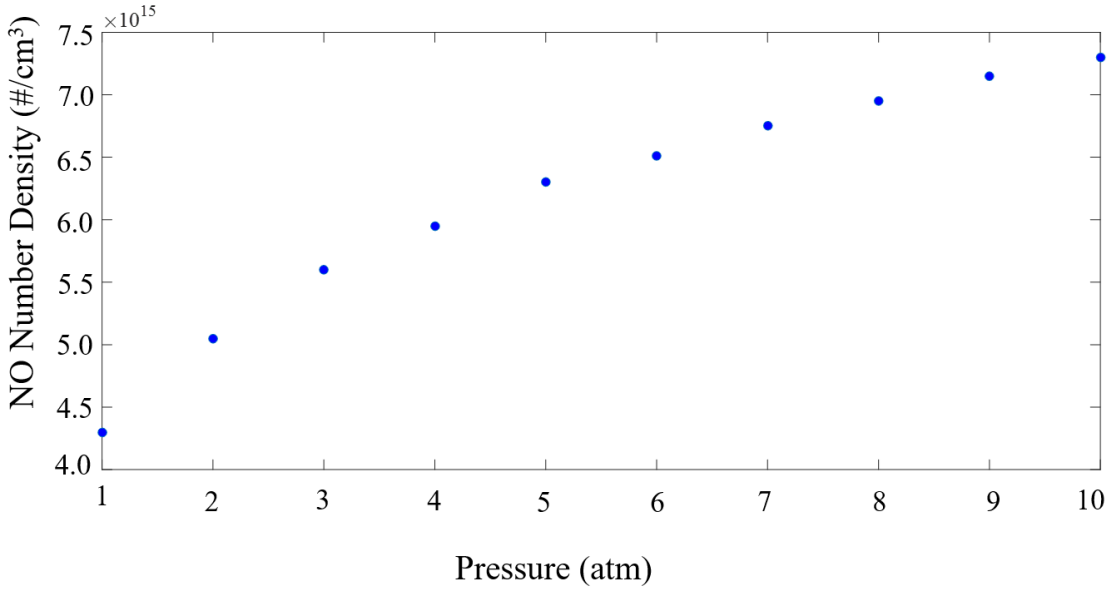

Figure 10: NO number density dependence on pressure at 300 K and 1% ionization. All data points taken 1 ms after simulation start at 1% ionization of N_2. Trend does not appear to be linear, however, increased pressure is correlated to increased NO levels.

Chapter 3: Experimental Setup and Procedure

A schematic for the experimental setup is pictured in figure 11. The "write" component of the system is a frequency tripled QuantaRay Nd:YAG system producing 355 nm output. The tripled output consists of ≈150 mJ, 10 ns pulsed 355 nm light operating at 10 Hz. The output beam is steered to a 250 mm focal length spherical plano-convex lens. The focused beam is close to the edge of the breakdown limit of air at the beam waist. The waist of the beam was centered in the 1 inch square outlet of a Hencken burner. For further study, a pressure vessel was used in place of the Hencken burner. Due to the geometry of the pressure vessel, the 250 mm focal length lens was impossible to use, and therefore a 1 m focal length spherical plano-convex lens was used. For these trials the beam was not riding the edge of the breakdown limit.

The "read" component of the MTV system consists of a frequency doubled Powerlite Nd:YAG (532 nm) pumping a Continuum dye laser utilizing Rhodamine 590 laser dye dissolved in methanol. The output of the dye laser (574 nm) is then doubled (287 nm) and mixed with the fundamental output of the Powerlite (1064 nm) in a wavelength extender (WEX) to produce the "read" laser of 226 nm. The 226 nm light excites the $A^2\Sigma^+(v'=0) \leftarrow X^2\Pi(v''=0)$ band of NO [12]. The pulse energy out of the WEX was measured at ≈0.5 mJ, however shot-to-shot fluctuations were of sufficient magnitude that reliable energy reading of the "read" beam were not possible. Fluctuations caused the energy to dip below the detectability threshold of the equipment. Therefore the magnitude of the fluctuations is not known, but the upper limit was 0.5 mJ. The WEX is equipped with tracking logic to match the optimum angle of the doubling crystal and mixing crystal relative to the incoming beam to maximize doubling and mixing efficiencies. The tracking logic for the doubling stage worked well. However, the low energy after the mixing state makes tracking

nearly impossible for the mixed output. Instead, the mixing crystal was hand tuned to optimal output. The 226 nm read beam was focused using a 500 mm focal length, cylindrical plano-convex lens in order to form a probing sheet. This lens also had to be substituted for a 1 m focal length lens for the pressure vessel work.

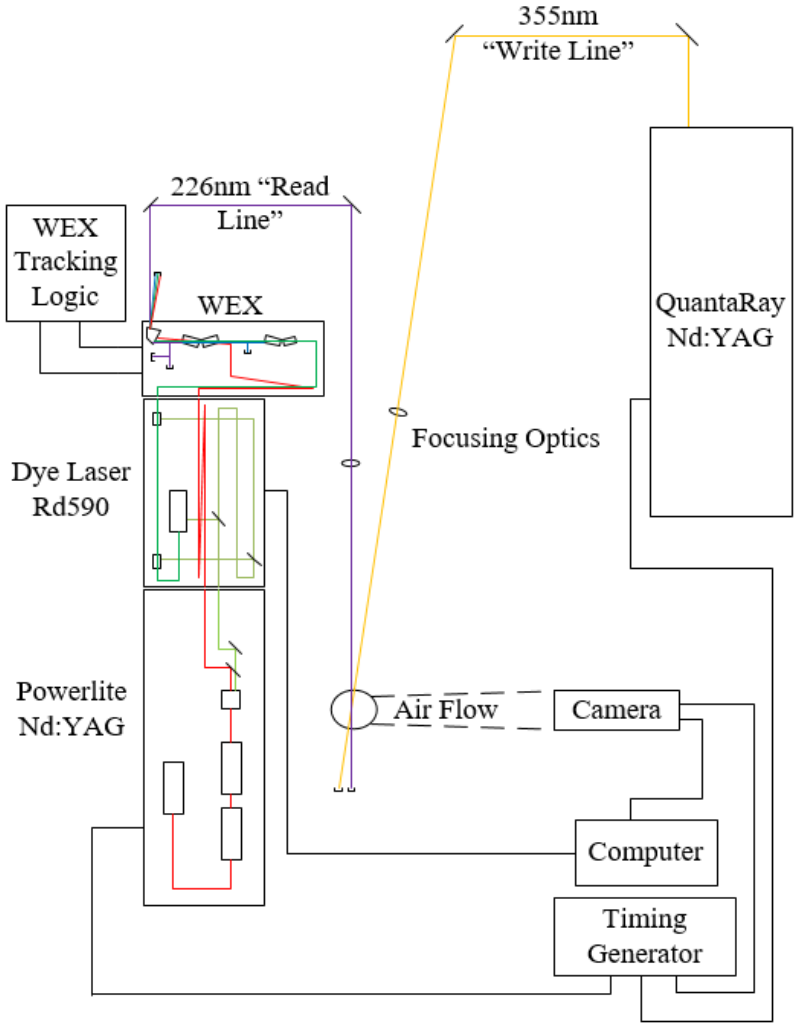

Figure 11: Experimental Schematic for tagging. The "read" system is pictured on the left and the "write" system on the right. Laser lines indicated by purple and yellow lines corresponding to the "read" and "write" beams respectively (226 nm and 355 nm). The internal system of the "read" laser shown indicated the various wavelengths produced and highlights the multiple stages of the laser, including 1064 nm, 532 nm, 574 nm, 287 nm, and finally 226 nm.

The Powerlite emits ≈0.5 J, 10 ns pulse of doubled output (532 nm) and ≈1 J, 10 ns pulse of fundamental output (1064 nm). Each successive stage operates at ≈10% efficiency (the dye laser outputs ≈50 mJ of 574 nm, the doubled output ≈5 mJ of 287 nm, and the mixed output ≈0.5 mJ of 226 nm). The approximate signs highlight the inefficiencies of the system (≈10% efficiency per stage) and reflect appropriate energy levels observed in the lab.

The camera used for imaging is a PI-MAX II ICCD camera equipped with a UG-5 filter to remove the incident 226 nm read light. NO has emission bands at 237 nm, 248 nm, and 259 nm [7]. These bands are transmitted through the UG-5 filter. The entire system is operated on 10 Hz with a Stanford Research Systems Model DG535 Digital Delay/Pulse Generator serving as the master clock for the system. The camera gate is opened 120 ns before the "read" sheet arrives over the burner and remains open for 1 μs. The field of view for the camera for the final images taken was a 40 mm square (over a 1024 pixel square) or 25.6 pixels per mm. The delay of the "read" sheet after the "write" line was varied from 1 μs to as much as 1 ms. This delay range was chosen because of previously observed NO tag at as little a delay as 1 μs on the short end, and the long lifetime of the NO making a significant delay (1 ms) possible as well. The shorter delays would be applicable in faster flows such as a sonic jet where the same mm scale displacement is achieved with a μs scale delay.

The viewing image is centered over a 1 inch square Hencken burner. For calibration runs the mixture flowed through the burner consisting of a N_2-NO mix with known values of NO. Then a series of experimental runs were performed with air flowing through the Hencken burner. The time delay was cycled through the range mentioned previously. However, NO was not detected in these experimental runs (excluding the calibration images). In order to maximize NO production (as the simulations projected), a pressure vessel was introduced into the beam path in place of the Hencken

burner. It measures 750 mm long with three 31 mm diameter optical access windows. The windows are 9.5 mm thick and made of fused silica. Two windows are perpendicular to the longitudinal axis for laser beam axis. The third window is parallel to the longitudinal axis in the middle of the presser vessel offering imaging access for the camera. This pressure vessel allowed for a study of the pressure dependency simulated previously. Moreover, after failing to observe NO formation above the Hencken burner, the pressure vessel offered the best case scenario to identify NO formation from the 355 nm “write” line. For the tagging images presented below, this pressure vessel was used. It has optical access for the “write” and “read” beams as well as for the camera.

CHAPTER 4: EXPERIMENTAL RESULTS

The first images taken were with the experimental setup shown in figure 1, with a Hencken burner installed in the viewing field and a N_2/NO mixture running through the burner at various concentrations in order to validate the "read" laser system and calibrate for the signal of the present NO. The gas mixture was from a high purity (>99%) N_2 bottle and a 1000 ppm NO (remainder N_2) bottle. The N_2 bottle was flowed at a constant 30 SLPM, while the NO mixed bottle was varied using a Hastings Teledyne Instruments 30 SLPM flow controller. The four cases examined are outlined in table 1. Where the collected signal and the relative signal (relative to the 3 SLPM flow case) are shown. The uncertainties in the number density arise from the uncertainties in the flow meter, which have a 1% of maximum flow rate uncertainty (i.e. 0.3 SLPM uncertainty). The corresponding images to these case are in figure 12 below. Figures 13 and 14 show an average cross section of the four cases presented in figure 12a-d. Each cross section is along the full 1024 pixel horizontal axis and is the average of 50 rows of pixels which correspond to a 2 mm high line centered on the peak intensity.

Table 1: NO Calibration runs and collected signal in arbitrary units. In all cases the NO was mixed with high purity N_2 flowing at 30 SLPM. Relative signal is compared to lowest signal case.

Volumetric Flow Rate (SLPM)	NO Concentration (ppm)	NO Number Density (#/cm^3)	Peak Intensity	Relative Signal
3	90	2.3 x10^{15} ± 9%	1468	1
6	170	4.2 x 10^{15} ± 4%	2121	1.445
15	340	8.32 x 10^{15} ± 1.5%	5119	3.487
30	510	1.25 x 10^{16} ± <1%	29942	20.397

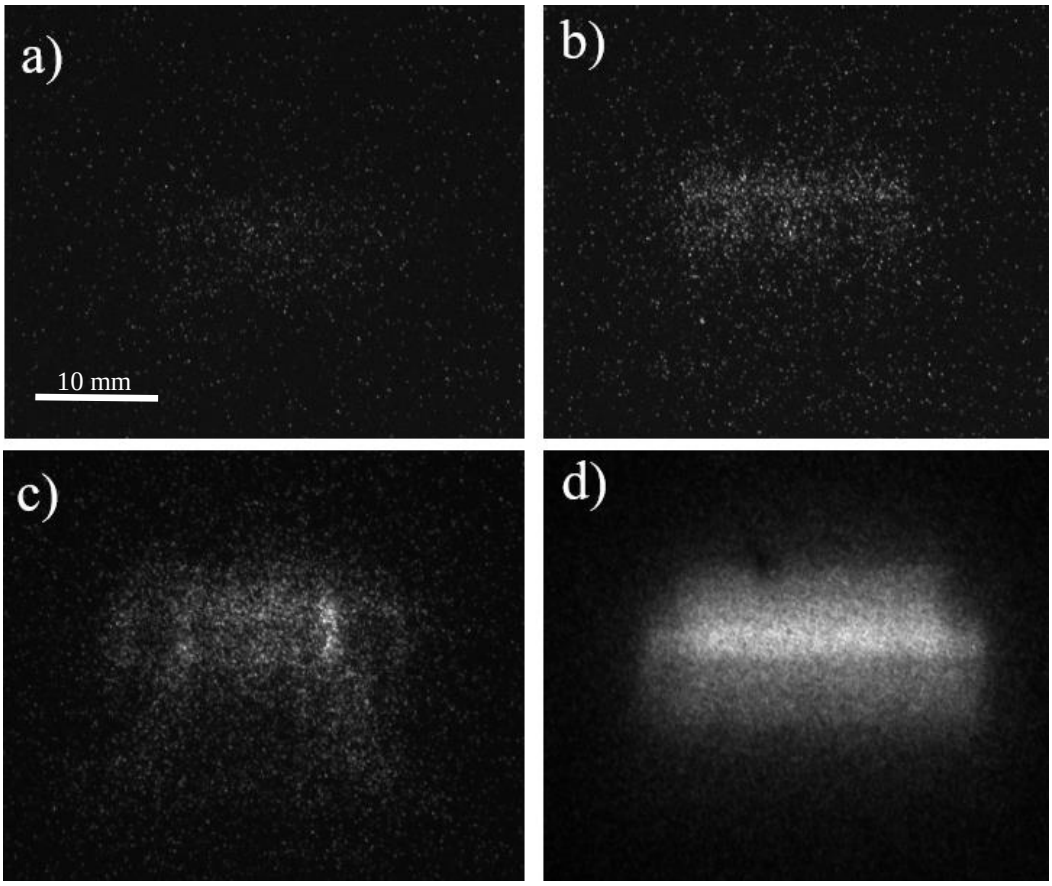

Figure 12: Raw images of NO fluorescence from NO mixed in N_2 corresponding to Table 1. Each image has a field of view approximately 50 mm square and is imaged at the exit of the Hencken burner. The fluid flows from bottom to top of the image. The images are 1024 x 1024 pixels in dimension. The "read" sheet is lifted off the burner by 25mm. a) 2.3×10^{15} #/cm^3 of NO, b) 4.2×10^{15} #/cm^3 of NO, c) 8.32×10^{15} #/cm^3 of NO, d) 1.25×10^{16} #/cm^3 of NO. The excitation wavelength for the LIF was 226 nm.

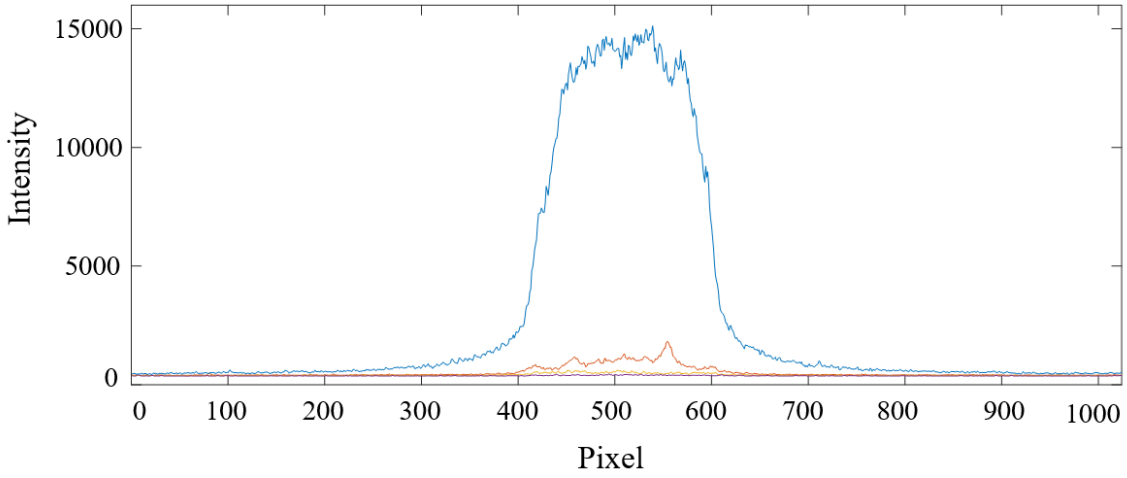

Figure 13: Intensity cross section of calibration images. Pixels represent the horizontal dimension. The intensity is the average intensity of a 50 pixel high section at each given horizontal pixel location. The data sets correspond to the images above (purple with image 12a, orange with image 12b, red with image 12c, and blue with image 12d). For clarity, figure 14 shows 12a-c in more detail with an appropriate intensity scale.

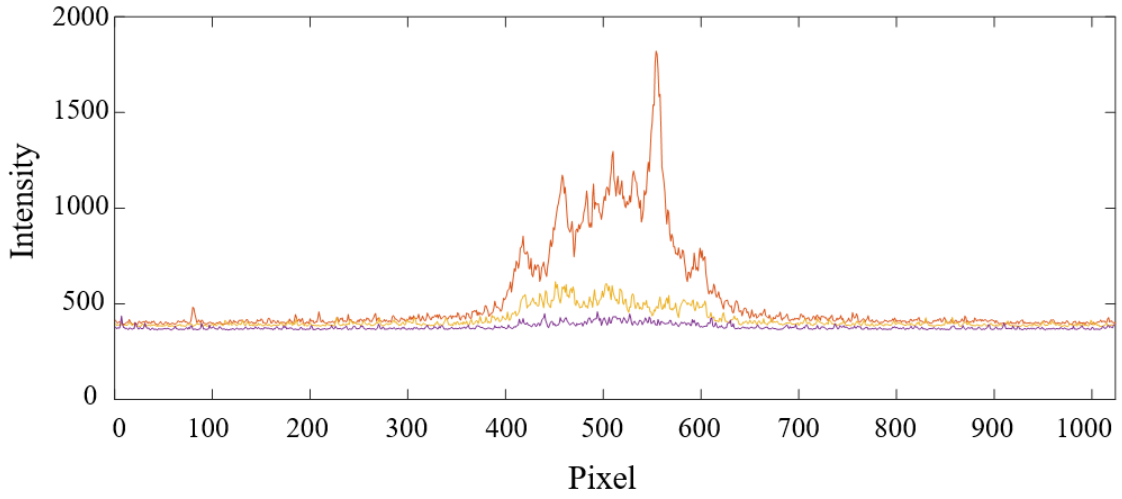

Figure 14: Enlarged image of figure 13 showing intensity cross sections of figure 12a-c. The legend provided in figure 13 is the same here (orange corresponds with image 12b, red with image 12c, and blue with image 12d).

After examining the bottled NO and finishing the "read" laser setup, images were attempted over the Hencken burner flowing air with the highly focused 355 nm "write" line writing a tag into the flow. However, no NO fluorescence was observable. At that point, a pressure vessel replaced

the Hencken burner in the camera's field of view to experimentally observe NO in the pressure conditions simulated in figures 5 and 6. The pressure of the air in the vessel was increased to the maximum safety limit of the vessel, 10 atm. The raw images presented in figure 15 were the result of this experimental run. The images show that the 355 nm "write" line did produce NO but at much lower levels than predicted with the assumption of 1% or 0.1% dissociation of N_2. The signal level of the image was 500 counts. This corresponds to about $7.7x10^{14}$ #/cm^3 (31 ppm) of NO, which is on the edge of detectability and well below the levels achieved in earlier work using 193 nm excitation. The predicted levels however, made the assumption of ionization levels, which have not been validated. Moreover, background signal intensity of the image was 400, making the SNR of the images 1.25. This SNR is from background NO and is not from each individual "write" pulse. Even if this SNR could be produced on a shot to shot basis of written lines it is still too low for practical use in MTV work [10].

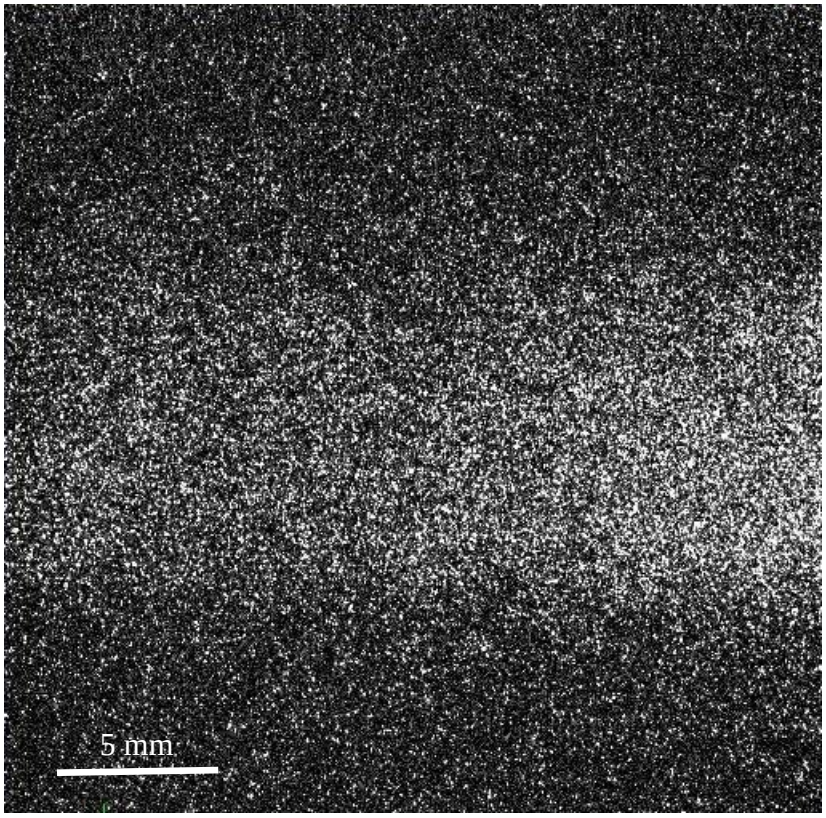

Figure 15: Pressure vessel raw image at 10 atm air, field of view approximately 15mm square. NO signal after 10 minutes running the 355 nm "write" beam through the pressure vessel (representing approximately 6000 laser pulses). Shows proof that NO is being generated and that it can be detected. However, NO production per laser pulse is so low that no distinct line from the 355 nm "write" process is visible. If production was higher a clear line, 0.2 mm wide (the diameter of the "write" beam) should be visible with a much higher signal than the accumulated background NO. Because this is not the case, only the diffuse NO is visible.

Ionization levels were not back calculated from the experimental images below using SENKIN because of the time delay involved with the images. As previously mentioned, these images were taken in the pressure vessel at 10 atm. The pressure vessel was not ventilated from shot-to-shot (impossible to evacuate the pressure vessel and then refill with 10 atm of air every 100 ms for the 10 Hz laser). Images were not taken operating the lasers in single shot mode. Therefore the images of NO fluorescence are of the gas in the vessel after being repeatedly exposed to the "write" beam. The long life of the NO (which makes it an ideal tag) also means that it does not fall apart in the pressure vessel even at 10 atm. Therefore, a stacking phenomenon occurred whereby each "write"

pulse ionized a small amount of N_2 which led to the creation of a small amount of NO. Every 100 ms a new “write” pulse created additional small amounts of NO. As this NO persisted, the stacking of multiple “write” pulses led to a buildup of NO. This means that although it has been shown conclusively that the 355 nm “write” laser did lead to the formation of NO, it is not possible from this work to observe or predict the ionization level per laser shot.

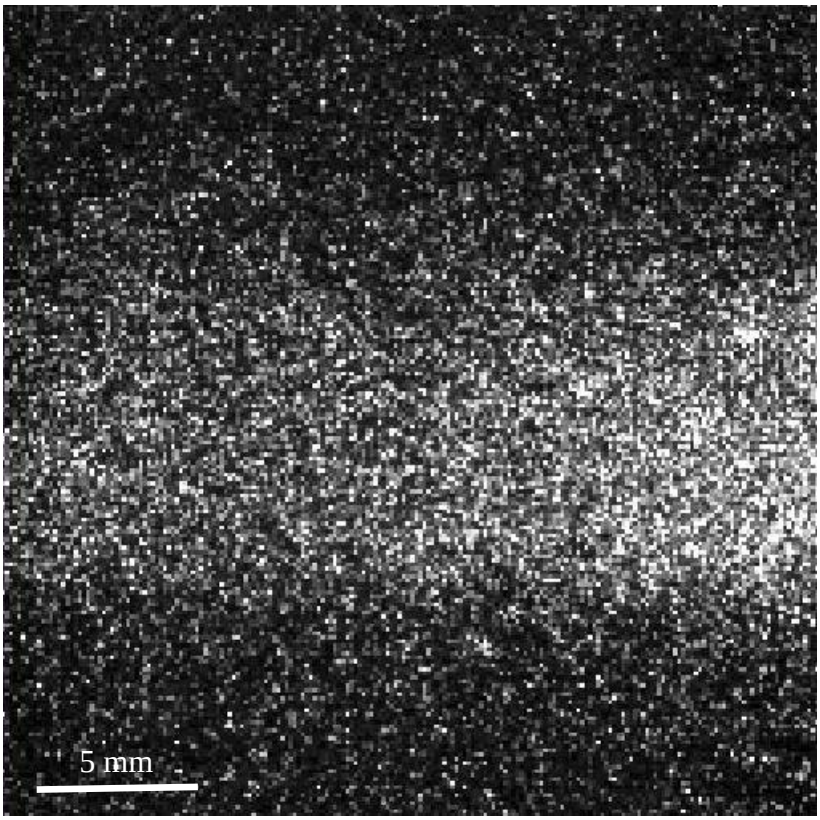

Figure 16: 5x5 binned image of previous figure. Spatial resolution is sacrificed for increased NO visibility.

CHAPTER 5: CONCLUSIONS

Ultimately, the goal of NO detection and production has been completed successfully. It has been shown that NO can be produced or "written" into air by focused 355 nm laser light, which has not been observed before. However, the conditions under which this was shown combined with the low signal and unusable SNR of the images at this point, precludes the use of NO produced by N_2^+ ionization via 355 nm light for MTV work. As is stands currently, either the SENKIN model using the Yetter mechanism [19] is inaccurate, or more likely the 355 nm excitation scheme is not as efficient as previously thought. The Yetter mechanism compares favorably with previous results, both in the amount of N_2^+ produced (measured in the waist region of a 193 nm ArF laser [12]) and the time of optimal signal generation (corresponding to peak NO levels observed at ≈ 5 μs [11]). Therefore the assumed ionization levels are too high in the simulation work, presented above, due to lower than expected efficiency of N_2 ionization with 6 photons of 355 nm light. The simulations have predicted several trends which are important to consider. First, the non-linear dependence of NO formation on ionization level of N_2. The ionization level is absolutely critical to the production of NO. Atomic nitrogen must have alternate consumption pathways that do not produce NO, such as recombination to form N_2. Unless photo-ionization of N_2 exceeds a certain level, NO will never be produced in high enough quantities for usable MTV work. The threshold levels of N_2 ionization for this experiment are discussed in more detail below. Second, due to the stable nature of NO, increased pressure enhances NO production without the drawback of a significant reduction in lifetime. Furthermore, increased pressure increases the number of N_2 molecules that are ionized (assuming the laser energy is not fully absorbed). That is to say, increased numbers of N_2 molecules are in the beam path of the laser and available to be ionized if enough beam energy is available.

The observed NO is so low that it is unusable for MTV. Previous work by Ramsey and Pitz have shown that a SNR of 4 is a threshold for MTV work due to constraints on accuracy [10]. Those results are shown in figure 17. In the experiments performed, a SNR of 1.25 was generated for the background NO created by ≈ 6000 355 nm laser pulses. However, this signal was of diffuse NO build up in the pressure vessel. "Written" lines were never imaged and therefore the more accurate SNR would be 0. No signal was generated directly from a "write" pulse, making MTV impossible.

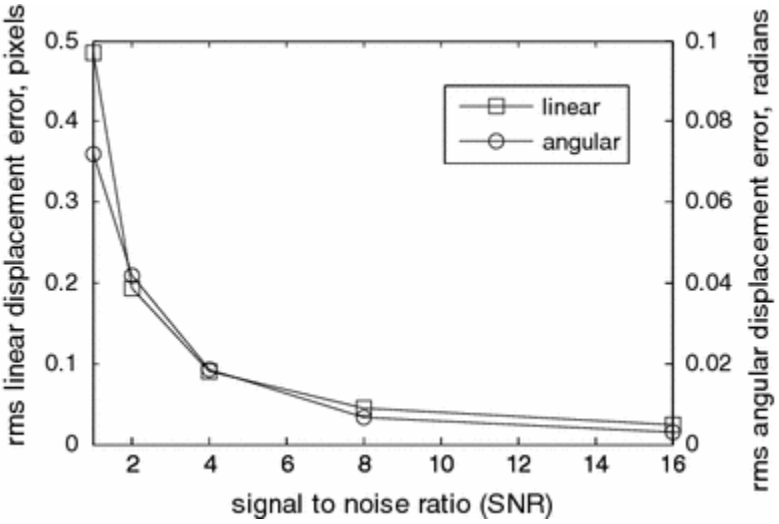

Figure 17: Reproduced figure from previous work by Ramsey and Pitz *[10]*. Graph shows linear and angular displacement errors as a function of the signal to noise ratio in an MTV system. A SNR of 1.25 (the highest SNR achieved through this work) would lead to an unacceptably high uncertainty in position and therefore velocity measurements in comparison to the 193 nm method.

SNR lower than this leads to unacceptably high uncertainties in the displacement measurement (measured by pixels). Therefore, even in the only case in which any NO was observed, the SNR is too low for use in an MTV system. Even if the SNR was high enough for an MTV study, the ionization level was not high enough to create enough NO from a single laser pulse. Without a "written" line, MTV is impossible. It is therefore the conclusion of this study that 355 nm ionization of N_2 is not efficient enough and therefore not practical for MTV work.

Figure 18 shows the SNR achieved in the calibration sets for the experimental setup used. Also included is a line of SNR value of 4. For the imaging setup utilized, a NO concentration of $3.45x10^{15}$ #/cm^3 is needed for accurate MTV work. Based on the simulation work presented in figure 8, the ionization threshold is 0.9% to achieve enough NO production for use.

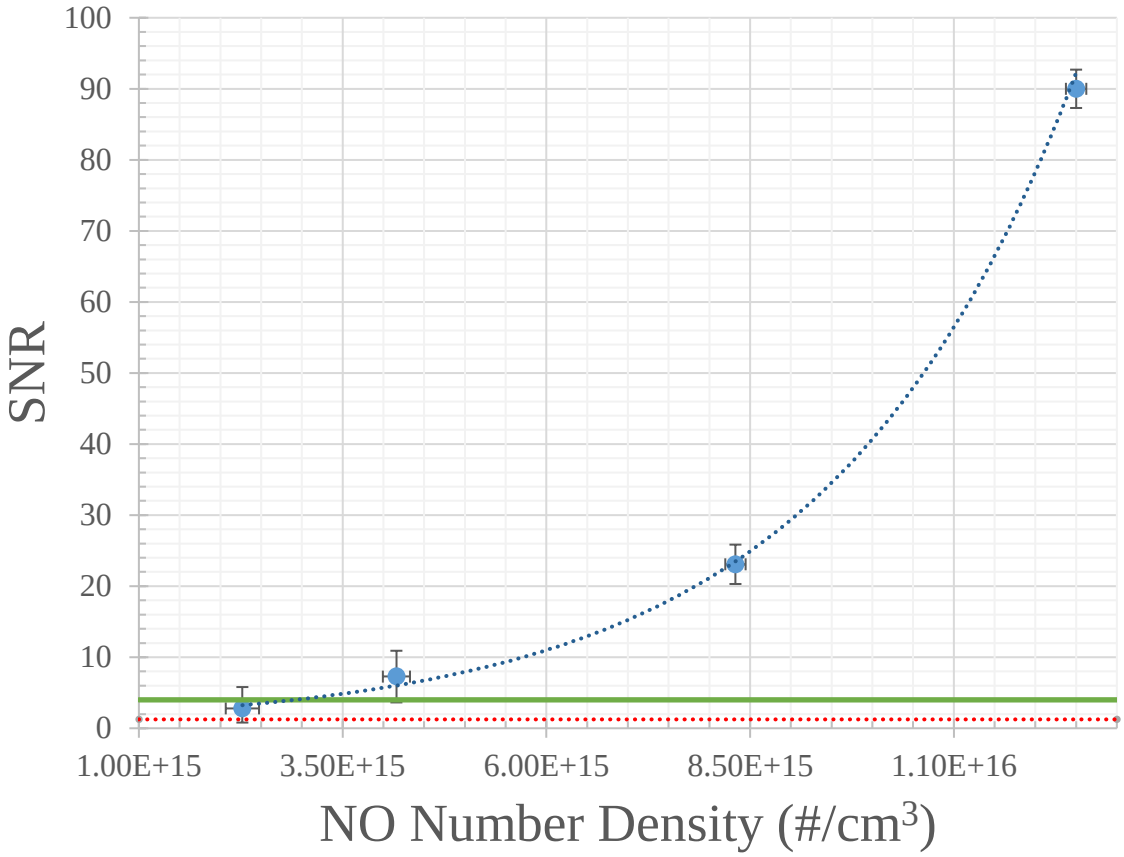

Figure 18: The SNR of each of the four calibration runs is plotted. The green horizontal line represents a SNR of 4, a commonly cited threshold for MTV work. The dashed red line if the SNR of the experimental run inside the pressure vessel at 10 atm. Using the trendline produced by the calibration data, a number density of $3.45x10^{15}$ #/cm^3 would be necessary to complete NO MTV. This value satisfies the SNR threshold of 4 and assumes the experimental setup ("read" laser and camera setup) remains unchanged.

The standard bearer of NO MTV is 193 nm N_2 ionization. Multiple studies have been performed on that topic, including the ones referenced in this paper [7] [11] [12] [16]. They have tracked NO MTV from the development to the maturity of the method. It was the ultimate goal of this study to provide an alternate and better ionization process for velocity measurements. It has

been determined that 355 nm ionization is not a solution to this problem. There may be alternate ways to form N_2^+ ions for NO work, but further study is needed.

CHAPTER 6: FUTURE WORK

Future work includes more examination into the mechanism of N_2 ionization. It may be possible for a direct comparison of N_2^+ ions in the waist regions of both a 193 nm beam and a 355 nm beam. In work by Nandula et al. [12], it is mentioned that N_2^+ can be observed via the $B^2\Sigma_u^+$ (v' = 0) → $X^2\Sigma_g^+$ (v" = 0) transition at 390 nm. The intensity of such signals being proportional to the level of N_2^+ ions produced. A further parametric study on the proportion of O_2 to N_2 could show that in some regimes, sufficient NO is produced for tagging use at 355 nm. This however would undermine the goal of having a MTV method for use in air. Alternative methods could be examined for NO production such as secondary creation pathways or alternative excitation schemes. If investigated, they may lead to NO tagging applications in air. Such examples could include use of a femtosecond laser or a frequency quadrupled Nd:YAG at 266 nm. Alternate pathways could also examine a variety of O_2 ionization or excitation schemes that could lead to NO production. The key to an oxygen path might be utilizing atomic oxygen in the ^1D state instead of the ^3P state. The ^1D state is much more reactive in the formation of bonds than the ^3P due to an empty space in the 2P orbital [21]. Studying ^1D formation both experimentally and in simulations is necessary before study into NO production in air via this pathway can be pursued.

REFERENCES

[1] B. J. McKeon, G. Comte-Bellot, J. F. Foss, J. Westerweel, F. Scarano, C. Tropea, J. F. Myers, J. W. Lee, A. A. Cavone, R. Schodl, M. M. Koochesfahani, D. G. Nocera, Y. Andreopoulos, W. J. Dahm, J. A. Mullin, J. M. Wallace, P. V. Vukoslavcevic, S. C. Morris, E. R. Paradyjak and A. Cuerva, "Velocity, Vorticity, and Mach Number," in *Springer Handbook of Experimental Fluid Mechanics*, Berlin Heidelberg, Springer, 2007, pp. 215-471.

[2] J. B. Michael, M. R. Edwards, A. Dogariu and R. B. Miles, "Femtosecond Laser Electronic Excitation Tagging for Quantitative Velocity Imaging in Air," *Applied Optics*, vol. 50, no. 26, pp. 5158-5162, 2011.

[3] M. M. Koochesfahani and D. G. Nocera, "Molecular Tagging Velocimetry," in *Handbook of Experimental Fluid Dynamics*, Springer-Verlag, 2007, pp. 362-382.

[4] C. Orlemann, C. Schulz and J. Wolfrum, "NO-Flow Tagging by Photodissociation of NO_2. A New Approach for Measuring Small-Scale Flow Structures," *Chemical Physics Letters*, vol. 307, no. 1-2, pp. 15-20, 1999.

[5] R. B. Miles, C. Cohen, P. Howard, S. Huang, E. Markovitz and G. Russel, "Velocity Measurements by Vibrational Tagging and Fluorescent Probing of Oxygen," *Optics Letters*, vol. 12, pp. 861-863, 1987.

[6] R. B. Miles, J. J. Connors, E. C. Markovitz, P. J. Howard and G. J. Roth, "Instantaneous Profiles and Turbulence Statitics of Supersonic Free Shear Layers by Raman Excitation Plus Laser-Induced Electronic Fluorescence (RELIEF)," *Experiments in Fluids*, vol. 8, pp. 17-24, 1989.

[7] N. M. Sijtsema, N. J. Dam, R. J. Klein-Douwel and J. J. ter Meulen, "Air Photolysis and Recombination Tracking: A New Molecular Tagging Velocimetry Scheme," *AIAA Journal*, vol. 40, no. 6, pp. 1061-1064, 2002.

[8] W. R. Lempert, P. Ronney, K. Magee, R. Gee and R. P. Haughland, "Flow Tagging Velocimetry in Incompressible Flow Using Photo-Activated Nonintrusive Tacking of Molecular Motion (PHANTOMM)," *Experiments in Fluids*, vol. 18, pp. 249-257, 1995.

[9] C. P. Gendrich and M. M. Koochesfahani, "A Spatial Correlation Technique for Estimating Veloctiy Fields using Molecular Tagging Velocimetry (MTV)," *Experiments in Fluids*, vol. 22, pp. 67-77, 1996.

[10] M. C. Ramsey and R. W. Pitz, "Template Matching for Improved Accuracy in Molecular Tagging Velocimetry," *Experiments in Fluids*, vol. 51, pp. 811-819, 2011.

[11] J. Bominaar, M. Pashtrapanska, T. Elenbaas, N. Dam, H. ter Meulen and W. van de Water, "Writing in Turbulent Air," *Physical Review*, vol. 77, no. 4, pp. 046312-1 - 046312-12, 2008.

[12] S. P. Nandula, R. W. Pitz, J. Bominaar, C. Schoemaecker, N. J. Dam and J. J. ter Meulen, "Kinetics of NO Tag Formation in Air for Unseeded Molecular Tagging Velocimetry," in *Aerospace Sciences Meeting*, Reno, 2004-390.

[13] R. Sanchez-Gonzales, R. D. Bowersox and S. W. North, "Simultanesous Velocity and Temperature Measurments in Gaseous Flowfields Using the Vibrationally Excited Nitric Oxide Monitoring Technique: A Comprehensive Study," *Applied Optics,* vol. 51, no. 9, pp. 1216-1228, 2012.

[14] R. Sanchez-Gonzales, R. D. W. Bowersox and S. W. North, "Vibrationally excited NO Tagging by $NO(A_2\Sigma^+)$ Fluorescence and Quenching for Simultaneous Velocimetry and Thermometry in Gaseous Flows," *Optics Letters,* vol. 39, no. 9, pp. 2771-2774, 2014.

[15] R. Sanchez-Gonzales, R. Srinivasan, R. D. Bowersox and S. W. North, "Simultaneous Velocity and Temperature Measurements in Gaseous Flow Field Using the VENOM Technique," *Optics Letters,* vol. 36, no. 2, pp. 196-198, 2011.

[16] N. Dam, J. H. Klein-Douwel, N. M. Sijtsema and J. J. ter Meulen, "Nitric Oxide Flow Tagging in Unseeded Air," *Optics Letters,* vol. 26, no. 1, pp. 36-38, 2001.

[17] W. van de Water and N. Dam, "How to Find Patterns Written in Turbulent Air," *Experiments in Fluids,* vol. 54, no. 1574, pp. 1-9, 2013.

[18] A. E. Lutz, R. J. Kee and J. A. Miller, "SENKIN: A FORTRAN Program for Predicting Homogeneous Gas-Phase Chemical Kinetics with Sensitivity Analysis," Sandia National Laboratories, Livermore, CA, 1988.

[19] L. A. Ribarov, J. A. Wehrmeyer, R. W. Pitz and R. A. Yetter, "Hydroxyl Tagging Velocimetry (HTV) in Experimental Air Flows," *Applied Physics B: Lasers and Optics,* vol. 74, pp. 175-183, 2002.

[20] S. Nagaraja, T. Li, J. A. Sutton, I. V. Adamovich and V. Yang, "Nanosecond Plasma Enhanced $H_2/O_2/N_2$ Premixed Flat Flames," *Proceedings of the Combustion Institute,* vol. 35, pp. 3471-3478, 2015.

[21] R. Y. N. Ho, J. F. Liebman, and J. S. Valentine, "Overview of Energetics and Reactivity of Oxygen," in *Active Oxygen in Chemistry,* Glasgow, Chapman and Hall, 1995, pp. 1-23.